

1
2
3
4
5
6
7
8
9
10
11
12
13
14
15
16
17
18
19
20
21
22
23
24
25
26
27
28
29
30
31
32

SUPPLEMENTAL DISCUSSION

Use of cell type-specific bulk sequencing versus single cell/nucleus sequencing

To characterize the distinct molecular states across post-embryonic development, we took a panoramic approach and profiled the transcriptome of the entire nervous system using INTACT technology^{14,55}. An alternative approach would be to use the rapidly advancing single cell sequencing technology, which would presumably give us single neuron resolution. We did not use this technology for the current study for practical (i.e. cost) and technical limitations (i.e. low capture rate/high drop-off rates for lowly expressed genes, difficulty of batch comparisons), although the rapidly evolving technology is starting to overcome some of these limitations. With our cell type-specific bulk sequencing, we were able to recapitulate previously described neuronally-enriched genes^{56,57}. In addition, our panneuronal profiling was able to capture all neuronal classes, as the top uniquely expressed genes in each neuronal class were well represented in our panneuronal IP data⁵⁸. We complemented our transcriptomic profiling with near perfect validation using gene expression reporter to extend our results to single neuron resolution, and identified many neuronal gene expression changes across post-embryonic development previously unknown (Extended Data Fig.2-4, Supplementary Table 6). However, our panneuronal profiling was less robust in identifying expression changes in small subsets of neurons among broadly expressing genes or those with opposite gene expression changes among subsets of neurons (i.e. *flp-14*), and could be supplemented in the future with complementary single-cell sequencing technologies

Developmental stage-specific molecular states for the nervous system

Our analysis of stage-specific transcriptomes warrants further discussion. A principal-component analysis (PCA) on the expression profile of these neuronally-enriched genes across post-embryonic developmental stages revealed that the neuronal transcriptome of each developmental stage clustered together and was distinct from the other stages, suggesting developmental stage-specific molecular states for the nervous system (Fig.1b, Extended Data Fig.1b-d). The two main principal components delineated the transitions between early larval (L1 and L2) stages and late larval (L4)/adult stages, and between all larval (L1 through L4) stages and the adult stage, respectively (Fig.1b, Extended Data

33 Fig.1b). This was further reiterated by the three major patterns of gene expression transitions
34 among these 2639 ($p_{\text{adj}} < 0.01$; ~33% out of the 7974 neuronally-enriched genes)
35 developmentally-regulated neuronally-enriched genes (Fig.1c, Supplementary Table 4, 5): 1)
36 cohorts of genes whose expression decreased across development, particularly from early
37 larval to late larval stages; 2) other cohorts of genes whose expression increased across
38 development, particularly during transition from early larval stages to late larval
39 stage/adulthood; 3) additional cohorts of genes whose expression peaked at the last larval
40 stage and subsequently decreased upon transition into adulthood. Additional principal
41 components revealed minor variations as a result of experimental batches (i.e. The increased
42 variabilities of L4 and adult samples were as a result of batch effect and was taken as a
43 variable for downstream analysis; Extended Data Fig.1c) and early larval stage specific
44 changes (i.e. L2; Extended Data Fig.1c). Comparison of differential gene expression across
45 all developmental transitions confirmed the general trends observed above (Extended Data
46 Fig.1h-j). Together, this data demonstrated that extensive molecular changes occurred during
47 post-mitotic post-embryonic neuronal development.

48 Temporal transitions in gene expression were prominently observed for molecules with
49 presumptive functions in neuronal communication. These included neurotransmitter receptors
50 and gap junction molecules (Extended Data Fig.2a, b), consistent with vertebrate reports of
51 altered chemical and electrical neurotransmission during postnatal development^{59,60}.
52 Perhaps the most striking changes were observed in the neuropeptidergic system, mostly on
53 the level of neuropeptide-encoding genes (Fig.1d, Extended Data Fig.3). The pervasive
54 expression change in the neuropeptide family across post-embryonic development, combined
55 with anecdotal evidence of dynamic neuropeptide expression controlling juvenile to adult
56 transitions across many organisms^{20,61-64}, suggest that altering the repertoire of
57 neuromodulatory peptides could be a conserved maturation mechanism in the animal
58 kingdom that define behavioral state transitions across development.

59 Another over-represented family of molecules amongst the developmentally-regulated
60 gene batteries is the cell adhesion molecules. This is consistent with reports of
61 developmental changes in the *C. elegans* connectome^{12,65}, and prompts future studies to
62 investigate the mechanisms by which changes in the expression of cell adhesion molecules
63 underlie developmental changes in the neuronal connectome. Additionally, the rich atlas of
64 post-embryonic molecular changes presented here could serve as a platform to understand

65 how previous reports of neurophysiology and behavior change during post-embryonic
66 development⁶⁶⁻⁷².

67

68 **Partial juvenization of the neuronal transcriptome by *lin-4* occurs through regulation of** 69 ***lin-14* and not *lin-28***

70 It is worth pointing out that *lin-4* and *lin-14* cannot be made responsible for all
71 developmental stage-specific changes in the neuronal transcriptome. Transcriptome profiling
72 revealed that *lin-4* null and *lin-14* gain of function mutations juvenized a subset of the
73 neuronal transcriptome in adults: 48% and 33% of genes that were upregulated and
74 downregulated, respectively, between the first larval and adult stage were juvenized by *lin-4*
75 null and/or *lin-14* gain of function mutations (Fig.2d, Extended Data Fig.6a-d, Supplementary
76 Table 7). *lin-14* gain of function mutation largely recapitulated the juvenizing effect of the *lin-4*
77 null mutation, as evidenced by PCA and correlational analysis (Extended Data Fig.6a-d),
78 demonstrating that *lin-4* acts through *lin-14* to affect the neuronal transcriptome.

79 Direct repression of the other well-characterized downstream effector of *lin-4*, the
80 conserved RNA-binding protein *lin-28/LIN-28*⁷³, did not account for any of the juvenizing
81 effect of *lin-4* null mutant on the adult neuronal transcriptome (Fig.2d, Extended Data Fig.6a-
82 d, Supplementary Table 7). This was expected, as deletion of the single *lin-4* repressive
83 binding site in the *lin-28* 3'UTR did not regulate the developmental downregulation of *lin-28*
84 (Extended Data Fig.6e). *lin-4* null and *lin-14* gain of function mutations delayed the
85 downregulation of *lin-28* (Extended Data Fig.6e), particularly across the L2->L3 transition,
86 and suggested that the previously characterized *lin-14* regulation of *lin-28*⁷⁴, rather than
87 direct repression by *lin-4*, likely mediated *lin-28*'s role in the mitotic progression of
88 hypodermal cells and sexual maturation^{15,69,70}. In the specific example of *nlp-45*, consistent
89 with the profiling experiments, *lin-28* gain or loss of function mutants did not affect its
90 developmental expression profile (Extended Data Fig.6e, 9a), suggesting that *lin-4* regulated
91 the maturation of the neuronal transcriptome largely through regulating the LIN-14
92 transcription factor.

93

94 **Previous characterization of the *lin-4/lin-14* in the nervous system and relevance to** 95 **vertebrate systems**

96 While our analysis represent the first nervous system-wide and unbiased analysis of
97 the effect of the heterochronic gene regulatory system on nervous system maturation, a
98 number of earlier studies have characterized the role of *lin-4/lin-14* in controlling the temporal
99 transitions in specific postmitotic neuronal cell types, demonstrating roles for this system in
100 synaptic rewiring, axonal extension/branching, synaptogenesis, sexual maturation of
101 postmitotic neurons and axonal degeneration^{69,70,72,75-81}.

102 The role of *lin-4* in controlling neuronal maturation appears to be conserved across
103 species, as *mir-125*, the *lin-4* ortholog, has been shown to control several aspects of
104 neuronal maturation in *Drosophila* and mice⁸²⁻⁸⁴. In humans, duplication or deletion of
105 chromosome 21 regions that include *mir-125* could result in intellectual and cognitive
106 disabilities, a phenotype that could be considered a maturation defect^{85,86}. Other microRNAs,
107 name *mir-101* and *mir-132* has previously been shown to regulate circuit activity maturation
108 and visual system maturation, respectively^{87,88}, indicating that microRNAs may be broadly
109 employed in the control neuronal maturation.

110

111 **Functional characterization of LIN-14**

112 Some aspects of our LIN-14 analysis warrant further discussion. The LIN-14
113 transcription factor is the main effector of *lin-4* microRNA regulated neuronal maturation.
114 Unlike other molecules in the heterochronic pathway, LIN-14 does not have an ortholog in
115 vertebrate based on sequence homology. Structure elucidation of LIN-14 could reveal
116 potential structural homology to known transcription factors in vertebrate. LIN-14 ChIP-seq
117 showed appreciable enrichment over input and wild type (N2) GFP ChIP-seq controls
118 (Extended Data Fig.8, 9). As expected for a transcription factor, the vast majority of LIN-14
119 binding were in genic regions, especially promoter regions (Extended Data Fig.8a, b). Motif
120 analysis identified YGGAR as a consensus binding sequence for LIN-14 (Extended Data
121 Fig.8a, b), which largely agreed with a previous characterization⁸⁹. Consistent with
122 decreased global level of LIN-14 protein across the L1->L2 transition (Extended Data Fig.5b),
123 there was a significant decrease in LIN-14 genomic binding across the same transition
124 (Extended Data Fig.8a,c, Supplementary Table 8-11). Despite over 3000 differential LIN-14
125 binding sites between L1 and L2 animals, less than 15% of those correlated with a change in
126 gene expression. One possible explanation could be due to the bulk nature of our

127 transcriptomic profiling that we could miss subtle cell type specific changes in gene
128 expression. Additionally, previous reports of ChIP-seq have shown that, for transcription
129 factors such as MyoD, the majority of bound sites are not functional and are usually
130 correlated with low occupancy levels⁹⁰. This is consistent with our analysis that showed that
131 for genes where LIN-14 acted as a repressor, as compared to genes where LIN-14 acted as
132 an activator or did not regulate gene expression, there was, on average, an increase in the
133 number of LIN-14 peaks within the genic area as well as an increase in peak enrichment
134 (Extended Data Fig.8d).

135

136 **References for Supplementary Discussion**

- 137 56 Kaletsky, R. *et al.* The *C. elegans* adult neuronal IIS/FOXO transcriptome reveals adult
138 phenotype regulators. *Nature* **529**, 92-96, doi:10.1038/nature16483 (2016).
- 139 57 Spencer, W. C. *et al.* A spatial and temporal map of *C. elegans* gene expression.
140 *Genome Res* **21**, 325-341, doi:gr.114595.110 [pii]10.1101/gr.114595.110 (2011).
- 141 58 Taylor, S. R. *et al.* Molecular topography of an entire nervous system. *Cell*,
142 doi:10.1016/j.cell.2021.06.023 (2021).
- 143 59 Laurie, D. J., Wisden, W. & Seeburg, P. H. The distribution of thirteen GABAA receptor
144 subunit mRNAs in the rat brain. III. Embryonic and postnatal development. *J Neurosci*
145 **12**, 4151-4172 (1992).
- 146 60 Nadarajah, B., Jones, A. M., Evans, W. H. & Parnavelas, J. G. Differential expression
147 of connexins during neocortical development and neuronal circuit formation. *J*
148 *Neurosci* **17**, 3096-3111 (1997).
- 149 61 Lee, G. *et al.* Developmental regulation and functions of the expression of the
150 neuropeptide corazonin in *Drosophila melanogaster*. *Cell Tissue Res* **331**, 659-673,
151 doi:10.1007/s00441-007-0549-5 (2008).
- 152 62 Wu, Q. *et al.* Developmental control of foraging and social behavior by the *Drosophila*
153 neuropeptide Y-like system. *Neuron* **39**, 147-161, doi:10.1016/s0896-6273(03)00396-9
154 (2003).
- 155 63 Conzelmann, M. *et al.* Conserved MIP receptor-ligand pair regulates *Platynereis* larval
156 settlement. *Proc Natl Acad Sci U S A* **110**, 8224-8229, doi:10.1073/pnas.1220285110
157 (2013).
- 158 64 Ellison, P. T. *et al.* Puberty as a life history transition. *Ann Hum Biol* **39**, 352-360,
159 doi:10.3109/03014460.2012.693199 (2012).
- 160 65 White, J. G., Albertson, D. G. & Anness, M. A. Connectivity changes in a class of
161 motoneurone during the development of a nematode. *Nature* **271**, 764-766 (1978).
- 162 66 Faumont, S., Boulin, T., Hobert, O. & Lockery, S. R. Developmental regulation of
163 whole cell capacitance and membrane current in identified interneurons in *C. elegans*.
164 *J Neurophysiol* **95**, 3665-3673, doi:10.1152/jn.00052.2006 (2006).
- 165 67 Fujiwara, M., Aoyama, I., Hino, T., Teramoto, T. & Ishihara, T. Gonadal Maturation
166 Changes Chemotaxis Behavior and Neural Processing in the Olfactory Circuit of

167 Caenorhabditis elegans. *Current biology : CB* **26**, 1522-1531,
 168 doi:10.1016/j.cub.2016.04.058 (2016).

169 68 Stern, S., Kirst, C. & Bargmann, C. I. Neuromodulatory Control of Long-Term
 170 Behavioral Patterns and Individuality across Development. *Cell* **171**, 1649-1662
 171 e1610, doi:10.1016/j.cell.2017.10.041 (2017).

172 69 Lawson, H. *et al.* The Makorin lep-2 and the lncRNA lep-5 regulate lin-28 to schedule
 173 sexual maturation of the C. elegans nervous system. *eLife* **8**, doi:10.7554/eLife.43660
 174 (2019).

175 70 Pereira, L. *et al.* Timing mechanism of sexually dimorphic nervous system
 176 differentiation. *eLife* **8**, doi:10.7554/eLife.42078 (2019).

177 71 Hale, L. A., Lee, E. S., Pantazis, A. K., Chronis, N. & Chalasani, S. H. Altered Sensory
 178 Code Drives Juvenile-to-Adult Behavioral Maturation in Caenorhabditis elegans.
 179 *eNeuro* **3**, doi:10.1523/ENEURO.0175-16.2016 (2016).

180 72 Olsson-Carter, K. & Slack, F. J. A developmental timing switch promotes axon
 181 outgrowth independent of known guidance receptors. *PLoS Genet* **6**,
 182 doi:10.1371/journal.pgen.1001054 (2010).

183 73 Moss, E. G., Lee, R. C. & Ambros, V. The cold shock domain protein LIN-28 controls
 184 developmental timing in C. elegans and is regulated by the lin-4 RNA. *Cell* **88**, 637-
 185 646 (1997).

186 74 Tzialikas, J., Romens, M. A., Abbott, A. & Moss, E. G. Stage-Specific Timing of the
 187 microRNA Regulation of lin-28 by the Heterochronic Gene lin-14 in Caenorhabditis
 188 elegans. *Genetics* **205**, 251-262, doi:10.1534/genetics.116.195040 (2017).

189 75 Howell, K., White, J. G. & Hobert, O. Spatiotemporal control of a novel synaptic
 190 organizer molecule. *Nature* **523**, 83-87, doi:10.1038/nature14545 (2015).

191 76 Hallam, S. J. & Jin, Y. lin-14 regulates the timing of synaptic remodelling in
 192 Caenorhabditis elegans. *Nature* **395**, 78-82 (1998).

193 77 Ritchie, F. K. *et al.* The Heterochronic Gene lin-14 Controls Axonal Degeneration in C.
 194 elegans Neurons. *Cell Rep* **20**, 2955-2965, doi:10.1016/j.celrep.2017.08.083 (2017).

195 78 Xu, Y. & Quinn, C. C. Transition between synaptic branch formation and
 196 synaptogenesis is regulated by the lin-4 microRNA. *Dev Biol* **420**, 60-66,
 197 doi:10.1016/j.ydbio.2016.10.010 (2016).

198 79 Zou, Y., Chiu, H., Domenger, D., Chuang, C. F. & Chang, C. The lin-4 microRNA
 199 targets the LIN-14 transcription factor to inhibit netrin-mediated axon attraction. *Sci*
 200 *Signal* **5**, ra43, doi:10.1126/scisignal.2002437 (2012).

201 80 Aurelio, O., Boulin, T. & Hobert, O. Identification of spatial and temporal cues that
 202 regulate postembryonic expression of axon maintenance factors in the C. elegans
 203 ventral nerve cord. *Development* **130**, 599-610 (2003).

204 81 Ivakhnitskaia, E., Hamada, K. & Chang, C. Timing mechanisms in neuronal
 205 pathfinding, synaptic reorganization, and neuronal regeneration. *Dev Growth Differ* **58**,
 206 88-93, doi:10.1111/dgd.12259 (2016).

207 82 Akerblom, M. *et al.* microRNA-125 distinguishes developmentally generated and adult-
 208 born olfactory bulb interneurons. *Development* **141**, 1580-1588,
 209 doi:10.1242/dev.101659 (2014).

210 83 Caygill, E. E. & Johnston, L. A. Temporal regulation of metamorphic processes in
 211 Drosophila by the let-7 and miR-125 heterochronic microRNAs. *Curr Biol* **18**, 943-950,
 212 doi:10.1016/j.cub.2008.06.020 (2008).

213 84 Wu, Y. C., Chen, C. H., Mercer, A. & Sokol, N. S. Let-7-complex microRNAs regulate
214 the temporal identity of *Drosophila* mushroom body neurons via *chinmo*. *Dev Cell* **23**,
215 202-209, doi:10.1016/j.devcel.2012.05.013 (2012).

216 85 Elton, T. S., Sansom, S. E. & Martin, M. M. Trisomy-21 gene dosage over-expression
217 of miRNAs results in the haploinsufficiency of specific target proteins. *RNA Biol* **7**, 540-
218 547, doi:10.4161/rna.7.5.12685 (2010).

219 86 Errichiello, E. *et al.* Dissection of partial 21q monosomy in different phenotypes:
220 clinical and molecular characterization of five cases and review of the literature. *Mol*
221 *Cytogenet* **9**, 21, doi:10.1186/s13039-016-0230-3 (2016).

222 87 Lippi, G. *et al.* MicroRNA-101 Regulates Multiple Developmental Programs to
223 Constrain Excitation in Adult Neural Networks. *Neuron* **92**, 1337-1351,
224 doi:10.1016/j.neuron.2016.11.017 (2016).

225 88 Mellios, N. *et al.* miR-132, an experience-dependent microRNA, is essential for visual
226 cortex plasticity. *Nat Neurosci* **14**, 1240-1242, doi:10.1038/nn.2909 (2011).

227 89 Hristova, M., Birse, D., Hong, Y. & Ambros, V. The *Caenorhabditis elegans*
228 heterochronic regulator LIN-14 is a novel transcription factor that controls the
229 developmental timing of transcription from the insulin/insulin-like growth factor gene
230 *ins-33* by direct DNA binding. *Mol Cell Biol* **25**, 11059-11072,
231 doi:10.1128/MCB.25.24.11059-11072.2005 (2005).

232 90 Biggin, M. D. MyoD, a lesson in widespread DNA binding. *Dev Cell* **18**, 505-506,
233 doi:10.1016/j.devcel.2010.04.004 (2010).

234

235

236

237

238

239

240

241

242

243

244

245

246

247

248

249

250

251

252

253

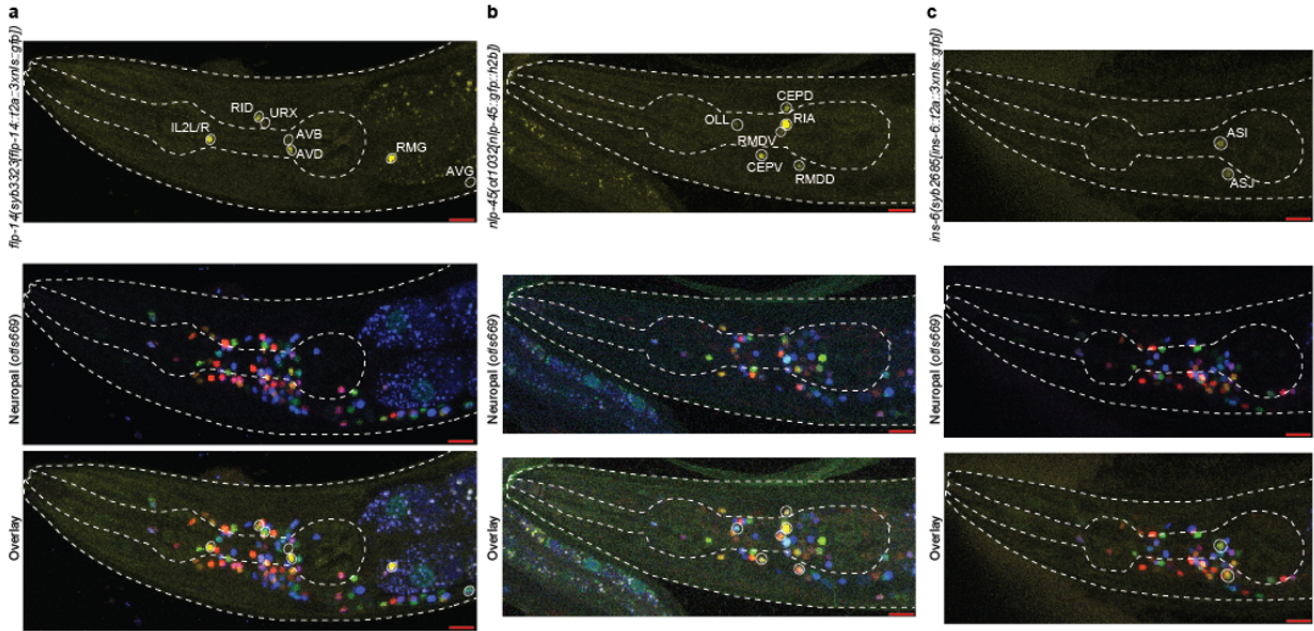
254

255

256

257

258 **Supplementary Fig.1 Using NeuroPAL to identify gene expression to single neuron**
 259 **resolution.** Representative overlay images of **a**, *flp-14*, **b**, *nlp-45*, and **c**, *ins-6* expression
 260 reporters with NeuroPAL are shown here. The top panels are the expression reporters by
 261 themselves (yellow). The middle panels are the NeuroPAL colors by themselves. The bottom
 262 is the overlay of the two for the identification of neuron types. Red scale bars (10µm) are on
 263 the bottom right of all representative images.
 264



265
 266

267 **SUPPLEMENTAL TABLES LEGENDS**

268

269 **Supplementary Table 1: Worm Tracking Summary**

270 Mean, standard deviation (S.D.), and standard error of mean (SEM) for each of the 726
271 parameters at each developmental stage are shown. The statistics (q(Wilcoxon)) for each
272 parameter and each comparison are also shown.

273

274 **Supplementary Table 2: Neuronally-enriched genes**

275 Comparison of neuronal-nuclei immunoprecipitated (IP) samples to input (total nuclei)
276 samples is conducted using DESeq2⁴² in R Studio to determine enrichment. 7974 genes
277 have a $\log_2\text{FoldChange} > 0$ (neuronally-enriched over input) and a $p_{\text{adj}} < 0.05$. The genes are
278 sorted by p_{adj} from smallest to largest. baseMean is the average normalized read counts of all
279 IP and input samples. $\log_2\text{FoldChange}$ is calculated using the formula $\log_2(\text{average read}$
280 $\text{counts of IP samples}) / (\text{average read counts of Input samples})$.

281

282 **Supplementary Table 3: Normalized read counts of all 7974 neuronally-enriched genes**
283 **across post-embryonic development**

284 Raw read count for the 7974 neuronally-enriched genes are extracted for the neuronal IP
285 samples and adjusted for library size. These are then used in DESeq2⁴² to conduct
286 comparisons between developmental stages, as shown in Supplementary Table 4-5. The
287 final read counts displayed are as a result of normalization done in the DESeq2 program.
288 There are 4, 5, 6, 7 replicates shown for L1, L2, L4, and adult stages respectively.

289

290 **Supplementary Table 4: Comparison of all temporal transitions among the 7974**
291 **neuronally-enriched genes across post-embryonic development.**

292 Pairwise comparisons between all stages are conducted using DESeq2⁴² as described in
293 Supplementary Table 2. The $\log_2\text{FoldChange}$ and p_{adj} are shown for each comparison. All
294 7974 neuronally-enriched genes are shown regardless of p_{adj} . The table is sorted
295 alphabetically by gene name.

296

297 **Supplementary Table 5: Normalized read counts of 2639 developmentally regulated**
298 **genes**

299 Same as Supplementary Table 3, but only with a subset of 2639 genes that have a $p_{\text{adj}} < 0.01$

300 in any pairwise comparisons between developmental stages.

301

302 **Supplementary Table 6: Developmental Change Summary**

303 Expression patterns, to single neuron resolution, for all validated reporters from Extended
304 Data Fig.2-4 are displayed here. The neurons that show expression for each gene at each
305 post-embryonic developmental stage (L1 through adult) are listed. Neurons in black do not
306 show altered developmental expression patterns while those labelled in green and red show,
307 respectively, decreases and increases in gene expression across development. Those
308 labelled in brown demonstrate both increases and decreases in expression across
309 development. d in brackets denote dim expression, m in brackets denote moderate level of
310 expression, while v in brackets denote variable expression.

311

312 **Supplementary Table 7: Genes that are juvenized in adult heterochronic mutants**

313 Pairwise comparisons between adult *lin-4(e912)* null, *lin-14(ot1149)* gain of function(gf), and
314 *lin-28(ot1154)* gf mutant neuronal IPs are conducted against adult control neuronal IP data,
315 using only the read counts of the 7974 neuronally-enriched genes. The \log_2 FoldChange and
316 p_{adj} are shown for each comparison. All 7974 neuronally-enriched genes are shown
317 regardless of p_{adj} . The table is sorted alphabetically by gene name. \log_2 FoldChange is
318 calculated using the formula $\log_2(\text{average read counts of mutant adult samples})/(\text{average}$
319 $\text{read counts of control adult samples})$.

320

321 **Supplementary Table 8: LIN14 ChIP peaks in L1 animals**

322 The 5 replicates from L1 animals are merged and the peaks are called using MACS2⁴⁶. The
323 ChIP-seq peaks are annotated to the nearest gene using CHIPseeker⁴⁷. Only the peaks
324 within 3kb of the closest genes are kept for this table. The peaks are arranged alphabetically
325 by the name of the closest associated gene.

326

327 **Supplementary Table 9: LIN14 ChIP peaks in L2 animals**

328 The 5 replicates from L2 animals are merged and the peaks are called using MACS2⁴⁶. The
329 ChIP-seq peaks are annotated to the nearest gene using CHIPseeker⁴⁷. Only the peaks
330 within 3kb of the closest genes are kept for this table. The peaks are arranged alphabetically
331 by the name of the closest associated gene.

332

333 **Supplementary Table 10: Differential LIN14 ChIP peaks between L1 and L2 animals as**
334 **determined by DiffBind**

335 Differential binding analysis between L1 and L2 samples is done using Diffbind⁴⁹. All
336 differential binding sites are annotated and assigned to the nearest gene using ChIPseeker
337⁴⁷. Only the peaks within 3kb of the closest genes are kept for this table. The peaks are
338 arranged alphabetically by the name of the closest associated gene.

339

340 **Supplementary Table 11: List of genes that exhibit differential LIN14 Binding during**
341 **L1->L2 transition**

342 This table contains the 3466 genes that show differential (mostly decreased) L1 vs L2
343 binding. This list is obtained using an amalgamation of different methods of assessing
344 differential LIN-14 binding across the L1->L2 transition, as detailed in Extended Data Fig.8c.
345 The genes are sorted alphabetically.

346

347 **Supplementary Table 12: Sexually dimorphic and dauer-induced expression patterns**
348 **of *lin-4/lin-14* controlled developmentally regulated genes.**

349 The sexually dimorphic and dauer-induced expression patterns of 5 genes (*nlp-45*, *flp-28*, *flp-*
350 *14*, *gcy-12*, *nlp-13*), that demonstrate *lin-4/lin-14* controlled developmental regulation, are
351 summarized in this table (For representative images, see Fig.3a, Extended Data Fig, 9). For
352 each gene, the neurons, whose developmental regulation is controlled by *lin-4/lin14*, are
353 listed in the second column. Those labelled in green and red show, respectively, decreases
354 and increases in gene expression across post-embryonic development in hermaphrodite
355 animals. Those labelled in blue gain expression in adult male animals, while those in orange
356 show additional expression upon entry into dauer. Those labelled in purple are regulated by
357 *lin-4/lin-14* but are not observed in any conditions tested in control animals. The neurons
358 where *lin-14* acts as a repressor or an activator are listed in the third and fourth column,
359 respectively. The last three columns show the neurons for each gene, whose expressions are
360 regulated across post-embryonic development in hermaphrodites, between adult males and
361 hermaphrodites, and between dauer and the comparable L3 mid-larval animals, respectively.
362 For most *nlp-45* expressing neurons and several *flp-14* expressing neurons, the sexually
363 dimorphic and dauer-specific expression patterns are consistent with regulation through *lin-*

364 14. #: For *flp-28*, the observation that these neurons, which show increased expression in
365 male and dauer animals, are consistent with the model that these expression patterns are
366 regulated through *lin-14*. However, due to the proximity of *flp-28* and *lin-14* locus, the *flp-28*
367 expression pattern couldn't be examined in *lin-14* null animals to determine the full battery of
368 neurons that demonstrate *lin-14* regulated *flp-28* expression. *: Sexually dimorphic or dauer-
369 specific expression patterns of *flp-14* for these neurons are not regulated through *lin-14*. †: No
370 obvious sexually-dimorphic and dauer-specific expression patterns are observed for *gcy-12*.
371 This could be due to the type of reporter (promoter fusion) and the diffuse (cytoplasmic)
372 signal of the reporter. Additional regulatory mechanisms that antagonize *lin-14* regulation of
373 *gcy-12* could also explain the lack of sexually-dimorphic or dauer specific expression pattern
374 of *gcy-12* in the ventral nerve cord motor neurons or elsewhere. ††: For *nlp-13*, the sexually
375 dimorphic and dauer-specific (no difference) expression patterns are not consistent with *lin-*
376 *14* regulation alone. This suggests additional *lin-14* independent regulatory mechanisms in
377 male and dauer animals. These data altogether suggest that although for some genes,
378 regulation through *lin-14* can largely explain the developmental, sexually-dimorphic, and
379 dauer-specific expression patterns. For other genes that are regulated by *lin-14*, there are
380 likely additional *lin-14* independent mechanisms that either synergize with or antagonize the
381 regulation by *lin-14*, leading to the complex expression patterns observed across temporal,
382 sexual and environmental dimensions of post-embryonic development.

383

384 **Supplementary Table 13: Strains Used in this manuscript**

385